Scientia Africana, Vol. 19 (No. 2), August, 2020. Pp 15-28
© Faculty of Science, University of Port Harcourt, Printed in Nigeria *ISSN 1118 – 1931*

AGBADA SANDSTONE WATER SATURATION: A FUNCTION OF CAPILLARY PRESSURE

Ugbena, K. G[1], Ogini, A. A[2], Ibrahim. S. O[1] and Ebeh. A[3]

[1]Department of Earth Sciences, Kogi State University Anyigba, Nigeria
[2]Department of Geology University of Benin, Nigeria
[3]Department of Geology University of Port Harcourt, Nigeria
Corresponding author: ugbenakelvins@yahoo.com
Tel: +2348032753119, +2348069123705

Received: 04-07-2020
Accepted: 19-08-2020

ABSTRACT

Analysis of representative reservoir rock specimen such as cores yields fundamental information for effective exploration, description and exploitation. Deliverability of particular reservoir sand can be estimated from measured permeability and residual fluid, oil, gas or water. Porosity and permeability values vary considerably within the Agbada formation, with generally high values. Studies of some basic reservoir parameters yield an insight into reservoir performance and establishment of a sound basis for estimation and exploitation. Results obtained from petrophysical analysis shows that the sandstones from the formation are unconsolidated. Core plugs used in this analysis were oven dried and saturated with a brine of synthetic concentration 44000ppm and resistance of 0.143Ωm to serve as the in-situ water saturation at 100%. Results show that the amount of water dropout from the core plugs is dependent on the capillary pressure as value increases from 1.00-60.00 psi. Saturation exponent values calculated using log RI/log Sw is also a function of the water saturation and capillary pressure. Resistivity Index values increases with increase in capillary pressure and decrease in water saturation. This is an indication that if oil is injected into these samples (formation), an ever increasing pressure will be required to push out the net bit of water which is the wetting phase. For a system under capillary/gravity equilibrium, water saturation will decrease with increase in capillary pressure. The amount of saturation water in a particular formation such as the Agbada formation reflects the resistivity response obtained under test and it is a function of capillary pressure. These parameters can be affected by increased burial, compaction and therefore indurations.

Keywords: Agbada formation, capillary pressure, reservoir, sandstone, water saturation

INTRODUCTION

Capillary pressure is a term that has been used to describe pressure differential between two immiscible fluid phases occupying the same pores caused by interfacial tension between the two phases that must be overcome to initiate flow (Fanchi, 2002, 2018; Dimri and Vedanti, 2012). Reservoir rock typically contains fluids of the immiscible phases; oil, water and gas. The forces that hold these fluids in equilibrium with each other and with the rock are expression of capillary forces. During water flooding, these forces may act together with frictional forces to resist the flow of oil. Capillary pressure concept can be used to model and evaluate parameters such as reservoir rock quality, expected fluid saturation, approximation of the recovery efficiency during primary or secondary recovery, thickness of transition zone (Charles *et al.*, 1992). Modeling of pressure and rate data is used to understand reserve/recovery potential and define reservoir characteristics (derive

mechanism, permeability, porosity, etc). Production data analysis provides key parameters to a series of reservoir engineering calculations such as reservoir estimation, inflow performance calculation and well production forecast (Milad *et al*., 2014). The ability to maximize the value of all the data, and to alter the geologic interpretation with ease, allows the initial characterization to provide enough information to next business decision. Achieving the maximum advantage of modeling in geology is realized with the full integration of different fields of study which includes; geophysics, petrophysics, electrical, sedimentology, reservoir engineering etc (Ugbena *et al.*, 2019).

The data required to described a reservoir and predict its production behavior is derived from a number of sources such as pressure-volume-temperature (PVT), Well test, mud returns, wire line log and conventional core analysis data. Using conventional approach (theoretical) to locate optimal location and trajectory of injection well is a lengthy process as the outcome is dependent on the ability to understand reservoir behavior and its operational limits (Mahmud and Liu, 2017). Analysis of representative reservoir rock specimen (cores) yields fundamental information for effective exploration, description and exploitation. This is because; Core data provides positive evidence of hydrocarbon presence (Oil or Gas) storage capacity (effective porosity). A few model studies however investigate the relationships between electrical properties and the geometric structure of a porous medium (Feng and Sen, 1985; Endres and Redman, 1996; Robert *et al*., 2006).

As part of the 3D characterization of a Tidal channel reservoir analog site in the Agbada Sandstone of the Niger Delta, formation evaluation is essentially performed on well-by-well basis. Capillary pressure in a reservoir determines the saturation distribution and hence the total *in-situ* volume of fluid (oil/water/gas). Water flow performance is also significantly affected by the capillary pressure of the rock (Masalmeh *et al.*, 2003). Therefore, having an accurate knowledge of the capillary pressure distribution on drainage is one of the primary factors in the reliable estimation of hydrocarbon reserves (Colin and Izaskun, 2015). Resistivity measurements along with porosity and water resistivity are used to obtain values of water saturation. Saturation values from shallow and deep resistivity measurement are compared in order to evaluate the productivity of a formation. Formation resistivity usually falls in the range from 0.2 to1000 ohm. m. Resistivity higher than 1000 ohm.m is uncommon in permeable formation. In many formations, resistivity may be very high except in permeable zones and in the shale (Schlumberger, 1972). Capillary pressure is the most fundamental rock/fluid property in multiphase flow, just as porosity and permeability are for single phase flow in oil and gas reservoir (Lake, 1989).

Geology of the Niger Delta

The Niger Delta Basin consists of Cenozoic formation and covers approximately 260,000km^2 (Chukwu *et al.*, 2007).The tertiary Delta is divided into three diachronous Formations (Fig. 1); Benin Formation consisting of Continental Sand, Agbada Formation consisting of Paralic Siliciclastics and the Akata Formation which consist of Marine Shales (Fig. 2). This division is in accordance with the sedimentation history. These Formations are recognized and categorized based on the basis of sand to shale ratio. The Akata Formation (Miocene to Recent) being the oldest of the Formations is estimated to be 7000m thick (Doust and Omatsola, 1990; Oladotun *et al.*, 2016). This Formation has been known to be the major source rock in the area. Agbada Formation (Eocene to Recent) is described as the major petroleum bearing reservoir which has been estimated

Scientia Africana, Vol. 19 (No. 2), August, 2020. Pp 15-28
© Faculty of Science, University of Port Harcourt, Printed in Nigeria *ISSN 1118 – 1931*

to be 3700m thick and forms the deltaic portion of the Niger Delta stratigraphic sequence. This siliciclasic sediment are known to be deposited in deltaic front, delta top set and fluvio-deltaic environment. The sand to shale ratio in the Agbada Formation decreases with increase in depth. The characteristics of the reservoir formation are strongly controlled by depositional environment and the depth of burial. Benin Formation (Oligocene to Recent) the youngest of the Formations, has thickness of over 2000m at some place in the delta. The fluvial and upper coastal plain facies that has been deposited since the Oligocene and, like the Akata and Agbada Formations, extends across the entire delta (Avbovbo, 1978). This Formation is known to host the water bearing zones and described as been prolific aquifer zone. Structures such as shale diapirs, growth faults, roll-over anticlines, steep dipping closely spaced flanks faults have been identified within the Niger Delta petroleum province. These structures are found below the Benin Formation (Merki, 1972; Weber and Daukoru, 1975; Evamy *et al.*, 1978; Xiao and Suppe, 1992; Avuru *et al.*, 2011).

Agbada Formation

The Agbada Formation, a coarsening upward sequence sediment overlying the Eocene Akata Formation was deposited over 6-7 million years during the middle to late Miocene. The Formation consists mainly of alternations of sands, sandstone and siltstones (Fig. 3). The sandy parts constitute the hydrocarbon reservoir which shows considerable lateral heterogeneity as a major characteristic of the Niger Delta oil fields (Nwachukwu and Chukwurah, 1986). The top of the Formation is at approximately 3000 feet below sea level at the base of freshwater sands. The base of the Formation is 8000 feet below sea level. It thickens basin wards towards the offshore depocenter (Hosper, 1971). Sandstones are the most common reservior rocks in the world and the main ones in the Niger Delta. Over 80% of the clastic grains are quartz. Because of variation and interlocking nature of the environment of deposition, Agbada Formation reserviors shows considerable heterogeneity. Porosity and permeability vary considerably, although values are generally high with porosity values of up 40% while permeability range between 1 to 2 Darcies (Davis and Ethridge, 1975). This is because the sandstones of the Formation are not well consolidated (Etu-Efeotor, 1997). Major characteristics of the Agbada Formation are controlled by depositional environment and by depth of burial (Evamy *et al*, 1978). Water saturation in the Agbada Formation is inversely proportional to the hydrocarbon saturation with water saturation decreasing with depth due ti increasing temperature (Ndip et al., 2018).

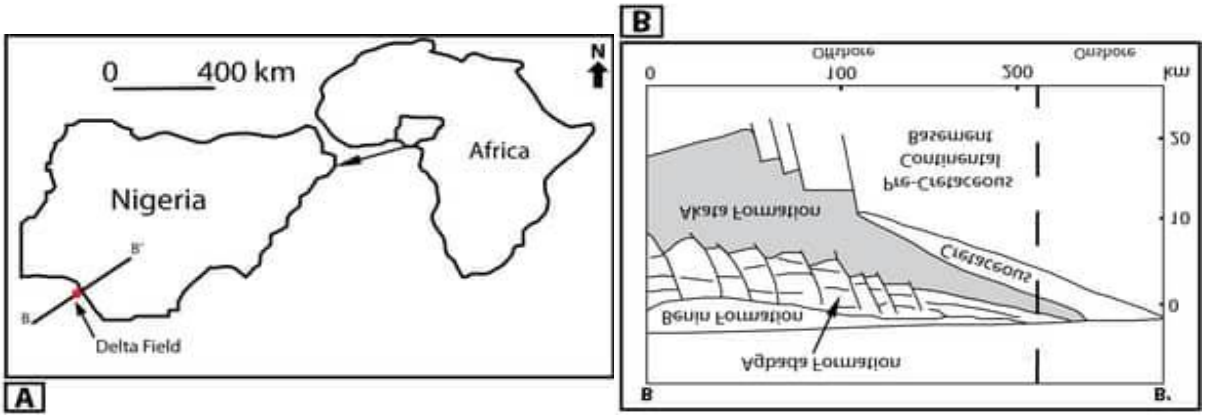

Fig. 1: A. Location of the Delta field, located within the Niger Delta. B. Cross section across the Niger Delta with depth in km (After Stacher, 1995).

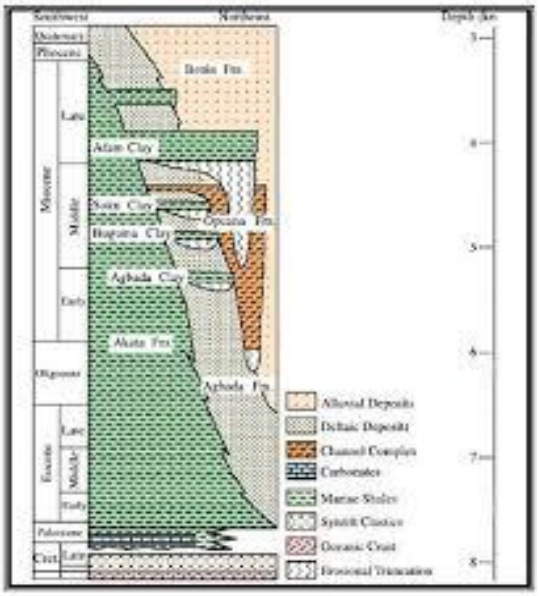

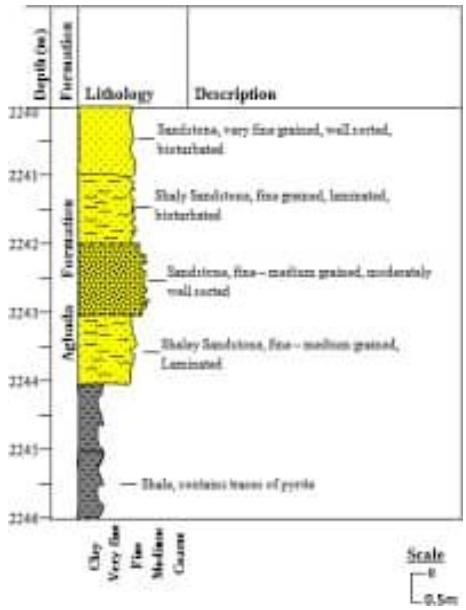

Fig. 2: Stratigraphic column showing the three Formations of the Agbada the Niger Delta (After Doust and Omatsola, 1990). (www.researchgate.net)

Fig. 3: Stratigrapic column of Formation (www.researchgate.net)

MATERIALS AND METHODS

This research relies on laboratory experimental results obtained from routine and special core analysis. In conducting the routine core analysis, properties such as porosity, permeability, and grain density of tested samples were determined, while formation factor, resistivity index, capillary pressure, water saturation data of the tested samples were determined during the special core analysis.

Core Slabbing and Plugging

Cores used were slab into two sections with thickness of 1/3 and 2/3 of the original diameter of the core. Plugs were extracted as close to one meter spacing as possible from the 2/3 section without regard for variations in lithrology. This is to ensure that data are measured on the most representative samples where the degree of heterogeneity is minimized or at least can be quantified. Plates 1 and 2

Plate 1: Core barrels

Plate 2: Extracted core plugs in metal tray

Scientia Africana, Vol. 19 (No. 2), August, 2020. Pp 15-28
© Faculty of Science, University of Port Harcourt, Printed in Nigeria *ISSN 1118 – 1931*

Core Cleaning and Plug Drying

Core cleaning was accomplished by means of hot solvents extraction (Soxhlett) techniques in which Toluene and Methanol were used to clean the samples of oil, water and salt. This was done below the boiling point of water to avoid the removal of water before the oil. In the laboratory, two basic methods were used to achieve this; Batch cleaning and the Dean-Stark methods. Using these methods, samples were first loaded in Soxhlett after pressuring them up to 400 psi. They were then batch cleaned in toluene which was heated to a temperature below the boiling point of water ($<100^0$c) to distilled the oil present in the samples until toluene was clean. Samples were then examined for evidence of staining and fluorescence. The solvent (toluene) was then changed to methanol and heated again to remove any salt present in the samples. The presence of salt was tested for using Silver trioxonitrate (V); $AgNO_3$. For the Dean stark, the samples already loaded into a rubber sleeve were loaded into the hydrostatic core holder with hand pump connected. The apparatus was then charged using clean toluene with the sample sealed to distill the solvent.

Distillation/Condensation helps to remove water from the solvent. The distilled water was collected in a receiving tube in which case, the volume can be monitored to determine the end point. This operation lasted for about eight hours with a periodic check. Distillation came to an end when stability in water volume reading was noticed. Samples were then weighed at the end of the cleaning process to determine weight difference before and after cleaning. Drying to constant weight was achieved using a conventional oven for a minimum of 24 hours at first and cooling to room temperature in a desiccator with samples in a metal tray (plate 2). Further drying was carried out with periodic check at every eight hours interval until constant weights were achieved when weights were repeated to plus or minus 0.01 gram for plug samples.

Capillary Pressure, Porous Plate Method (Air-brine) System

Core samples were first de-saturated with air using an evacuation pump for12 hours (all night). Samples were then saturated with brine of known concentration (the samples were weighed after de-saturation and after saturation with brine) for minimum of 8 hours and stored in a saturant bath. Archimedes BV, GV and saturated VP were determined and recorded. Placing one endstem at the end of the rubber boot ensuring that it is straight in the boot with at least 2mm of the boot showing above the end stem, a silver membrane was placed into the boot onto the endstem and pressed down to ensure all air is removed. A porous plate was inserted into the boot with a filter paper on it to ensure a good capillary content. Sample was removed from the storage brine, weighed ('weight in') and loaded into the boot and pushed to the endstem carefully. The second silver membrane was then placed on the sample before the second endstem carefully to ensure that all air was pushed out (plate 3).

Mounted sample was loaded into the Hydrostatic core holder with the end cap over the endstem and carefully pushed down leaving a small gap between the end cap and core holder to allow for oil to be poured into the core holder with all valves opened for a free flow of oil without pressure on the cell. Closing the pressure released valve, a confining pressure was pumped up into the cell. The temperature, resistance at 1 KHZ frequency across the sample was measured and recorded. Formation Factor "FF" and phase angle were calculated using the Arp's temperature conversion. Graduated pipette was then filled with brine up to a level of approximately $0.4cm^3$ in place on the top endstem, the "initial pipette reading" was recorded.

The pressure of the system was then increased to the next level and left to stabilize for 2 to 4 hours. When the reading was stable the "final pipette reading" was recorded noting the measured temperature and resistance readings on the equipment. The pressure was then increased to the next test pressure specified and left to stabilize for 24 hours. The above steps were repeated for each confining pressure increase and the formation factor FF was calculated for each sample using the formula (equations) (Plate 4).

Plate 3: Sample in a Rubber boot with endstems

Plate 4: Resistivity core holder and Digibridge

Resistivity Index Measurement

Resistivity index is the ratio of the resistivity of the partially saturated sample to the resistivity of the 100% saturated sample and is a function of water saturation. Resistivity index measurement was carried out using the same equipment for the determination of the formation factor, with the same sample loaded on the porous plate. Closing the cell carefully, humidified air was connected to the valve on the lid through a pressure source. Pressure was maintained until equilibrium was reached and this was achieved by monitoring the movement of the meniscus in the micro-pipette attached to the drain line.

The saturation at each step from the measurement weights was calculated. The saturation of the cores is determined by weights. The water saturation at any point is given by:

$$Sw = \frac{(\text{sample weight} - \text{dry weight}) * 100}{(\text{Saturated weight} - \text{dry weight})} \quad (1)$$

$$\text{Saturation Index Exponent} = n = -\log (RI)/\log (Sw) \quad (2)$$

$$\text{Resistivity Index} = RI = Rt/Ro \quad (3)$$

Capillary Pressure at Constant Stress

An overburden pressure of 2900 psig was applied to the brine-saturated plug sample loaded into the resistivity core holder with the saturated porous plate loaded at the downstream end for capillary measurements. Humidified air (which is the non-wetting phase) was used as the displacing fluid. Saturation at each capillary pressure point (0psig, 1psig, 5psig, 10psig, 20psig, 40psig and 60psig) was measured until both saturation and electrical equilibrium is reached. Saturation equilibrium at each pressure level were ascertained when the volume of the brine displaced remain constant. The cell pressure was increase to the next desired pressure point at equilibrium. Capillary pressure is calculated as follows:

$$Pc = Pd\ (Sw^*)\ 1/\lambda \quad (4)$$

Scientia Africana, Vol. 19 (No. 2), August, 2020. Pp 15-28
© Faculty of Science, University of Port Harcourt, Printed in Nigeria *ISSN 1118 – 1931*

$$\text{Log } Pc = \log Pd - 1/\lambda \log Sw^* \quad (5)$$

Where:

$Sw^* = (Sw-Swir)/(1-Swir)$

Swir = irreducible water saturation

Pc = capillary pressure

Sw^* = normalized water saturation

$\lambda = 1/m$ = pore size distribution index

m = absolute value of the slope of best fit line

Pd = displaced pressure

Results

Table 1: Water Saturation Measurement in Conjunction with Porous Plate Capillary Pressure

Synthetic formation Brine concentration = 44000ppm.

Sample Number	Depth (meter)	Confining Pressure (psi)	Permeability (mD)	Porosity (fraction)	Formation Resistivity Factor (FF)	Capillary Pressure (psi)	Water Sat, Sw (frac)	Formation Resistivity Index (RI)	Saturation Exponent (n)
01	2526.25	500	3100	0.337	4.63	0.00	1.000	-	
		2900		0.314	5.52	0.00	1.000	1.00	
						1.00	0.981	1.03	-1.72
						5.00	0.567	4.19	-2.53
						10.00	0.437	11.13	-2.91
						20.00	0.418	13.39	-2.97
						40.00	0.402	17.17	-3.12
						60.00	0.395	19.14	-3.17

Table 2: Water Saturation Measurement in Conjunction with Porous Plate Capillary Pressure
Synthetic formation Brine concentration = 44000ppm.

Sample Number	Depth (meter)	Confining Pressure (psi)	Permeability (mD)	Porosity (fraction)	Formation Resistivity Factor (FF)	Capillary Pressure (psi)	Water Sat, Sw (frac)	Formation Resistivity Index (RI)	Saturation Exponent (n)
02	2528.06	500	304	0.291	9.81	0.00	1.000	-	
		2900		0.276	10.91	0.00	1.000	1.00	
						1.00	0.965	1.02	-0.56
						5.00	0.705	1.82	-1.71
						10.00	0.572	3.12	-2.04
						20.00	0.484	4.19	-1.97
						40.00	0.465	4.73	-2.03
						60.00	0.471	4.80	-2.08

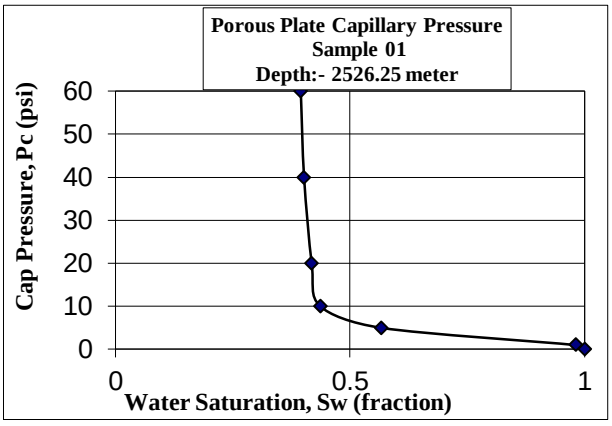

Figure 4: Capillary pressure versus water saturation

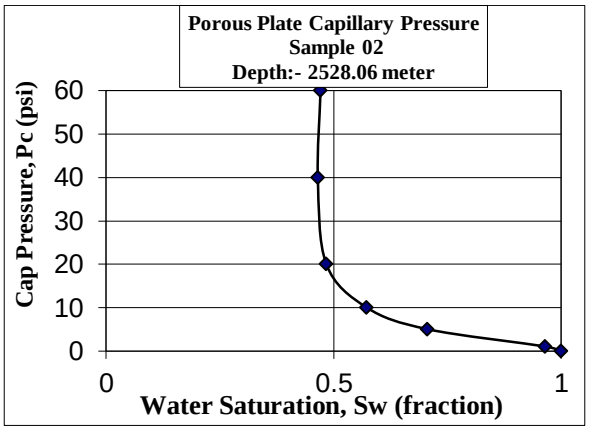

Figure 5: Capillary pressure versus water saturation

Table 3: Water Saturation Measurement in Conjunction with Porous Plate Capillary Pressure
Synthetic formation Brine concentration = 44000ppm.

Sample Number	Depth (meter)	Confining Pressure (psi)	Permeability (mD)	Porosity (fraction)	Formation Resistivity Factor (FF)	Capillary Pressure (psi)	Water Sat, Sw (frac)	Formation Resistivity Index (RI)	Saturation Exponent (n)
03	2530.28	500	2530	0.344	5.47	0.00	1.000	-	
		2900		0.337	6.10	0.00	1.000	1.00	
						1.00	0.968	1.01	-0.31
						5.00	0.192	29.99	-2.06
						10.00	0.114	71.72	-1.97
						20.00	0.089	96.67	-1.89
						40.00	0.086	114.85	-1.93
						60.00	0.078	122.75	-1.89

Table 4: Water Saturation Measurement in Conjunction with Porous Plate Capillary Pressure
Synthetic formation Brine concentration = 44000ppm.

Sample Number	Depth (meter)	Confining Pressure (psi)	Permeability (mD)	Porosity (fraction)	Formation Resistivity Factor (FF)	Capillary Pressure (psi)	Water Sat, Sw (frac)	Formation Resistivity Index (RI)	Saturation Exponent (n)
04	2532.30	500	4930	0.381	5.67	0.00	1.000	-	
		2900		0.390	7.02	0.00	1.000	1.00	
						1.00	0.957	1.10	-2.17
						5.00	0.672	3.30	-3.42
						10.00	0.351	62.38	-3.95
						20.00	0.272	80.66	-3.37
						40.00	0.267	98.54	-3.48
						60.00	0.259	108.02	-3.47

Scientia Africana, Vol. 19 (No. 2), August, 2020. Pp 15-28
© Faculty of Science, University of Port Harcourt, Printed in Nigeria *ISSN 1118 – 1931*

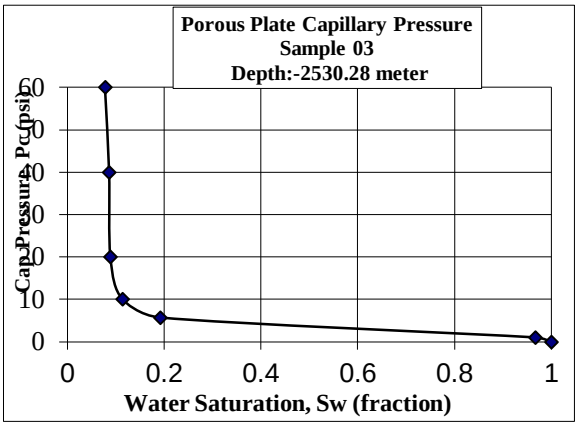

Figure 6: Capillary pressure versus water saturation

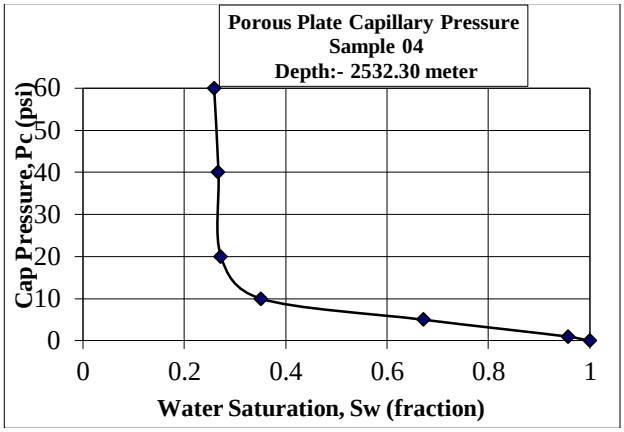

Figure 7: Capillary pressure versus water saturation

Table 5: Water Saturation Measurement in Conjunction with Porous Plate Capillary Pressure
Synthetic formation Brine concentration = 44000ppm.

Sample Number	Depth (meter)	Confining Pressure (psi)	Permeability (mD)	Porosity (fraction)	Formation Resistivity Factor (FF)	Capillary Pressure (psi)	Water Sat, Sw (frac)	Formation Resistivity Index (RI)	Saturation Exponent (n)
05	2534.32	500	3330	0.348	5.58	0.00	1.000	-	
		2900		0.333	6.01	0.00	1.000	1.00	
						1.00	0.978	1.03	-1.33
						5.00	0.567	2.66	-1.72
						10.00	0.130	40.00	-1.81
						20.00	0.057	113.50	-1.65
						40.00	0.047	125.44	-1.58
						60.00	0.042	135.37	-1.56

Table 6: Water Saturation Measurement in Conjunction with Porous Plate Capillary Pressure
Synthetic formation Brine concentration = 44000ppm.

Sample Number	Depth (meter)	Confining Pressure (psi)	Permeability (mD)	Porosity (fraction)	Formation Resistivity Factor (FF)	Capillary Pressure (psi)	Water Sat, Sw (frac)	Formation Resistivity Index (RI)	Saturation Exponent (n)
06	2536.26	500	2560	0.359	5.20	0.00	1.000	-	
		2900		0.341	6.43	0.00	1.000	1.00	
						1.00	0.952	1.02	-0.43
						5.00	0.448	3.81	-1.67
						10.00	0.209	23.70	-2.02
						20.00	0.108	61.35	-1.85
						40.00	0.093	69.26	-1.79
						60.00	0.084	83.23	-1.78

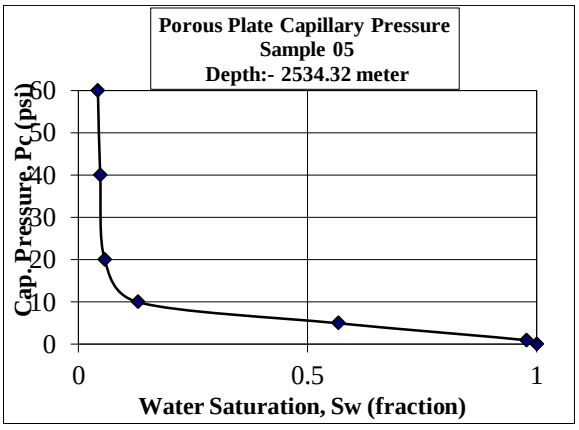

Figure 8: Capillary pressure versus water saturation

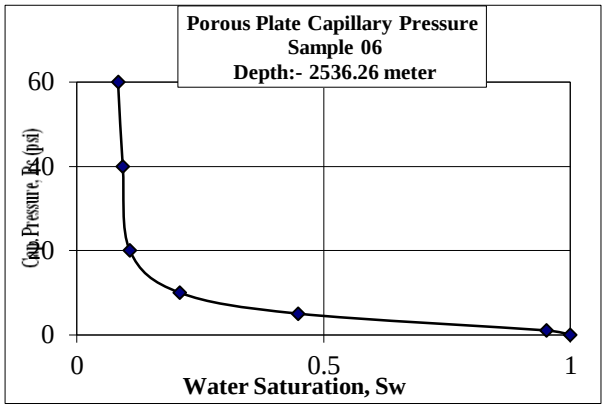

Figure 9: Capillary pressure versus water saturation

Table 7: Water Saturation Measurement in Conjunction with Porous Plate Capillary Pressure
Synthetic formation Brine concentration = 44000ppm.

Sample Number	Depth (meter)	Confining Pressure (psi)	Permeability (mD)	Porosity (fraction)	Formation Resistivity Factor (FF)	Capillary Pressure (psi)	Water Sat, Sw (frac)	Formation Resistivity Index (RI)	Saturation Exponent (n)
07	2538.29	500	2410	0.334	6.18	0.00	1.000	-	
		2900		0.378	6.74	0.00	1.000	1.00	
						1.00	0.982	1.03	-1.54
						5.00	0.591	2.69	-1.88
						10.00	0.340	7.62	-1.88
						20.00	0.139	31.76	-1.75
						40.00	0.121	35.03	-1.68
						60.00	0.109	38.02	-1.64

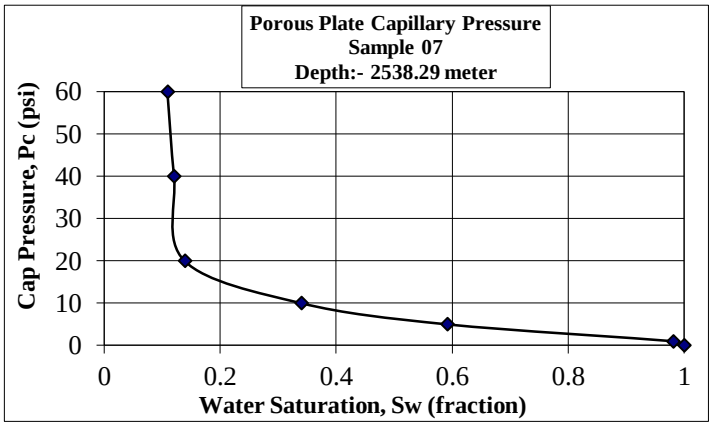

Figure 10: Capillary pressure versus water saturation

DISCUSSION

Formation resistivity factor increases with increase in confining pressure from 500-2900 psi and capillary pressure from 1.00-60.00 psi for all plugs as fluid content is lost due to increasing pressure. Formation factor is the basic measurement for reservoirs fluid saturation and is a function of porosity, type of fluid (i.e. hydrocarbon, salt or fresh water) and type of rock. Saturation exponent (n), models the dependence on the non-conductive fluid (hydrocarbons) in the pore space and it is related to the wettability of the rock. Water-wet rocks will for low water saturation values maintain a

Scientia Africana, Vol. 19 (No. 2), August, 2020. Pp 15-28
© Faculty of Science, University of Port Harcourt, Printed in Nigeria *ISSN 1118 – 1931*

continuous film along the pore walls making the rock conductive, while oil-wet rocks will have discontinuous droplet of water within the pore spaces making the rock less conductive. Results show that saturation exponent values calculated using log RI/log Sw vary as a function of the water saturation and capillary pressure as represented in Tables 1-7. The amount of water dropout from the core plugs is dependent on the test capillary pressure as it increases from 1.00-60.00 psi. Resistivity Index increases with increase in capillary pressure and with decrease in water saturation from 100% to lesser values as more water is pushed out making the samples more resistive to electrical current passing through (Tables 1-7 and Figures 4-10).

Capillary pressure (PC) which is the pressure difference between the non-wetting phase and the wetting phase is a function of the (wetting phase) saturation. For oil/water system in a porous medium, oil is generally considered to be the least wetting phase. From the results on the Tables and plots, it shows that with capillary pressure rising to very high values, 1.00-60.00 psi, there is decrease in water saturation. This is an indication that if oil is ejected into this system, an ever injection pressure will be required to force the net bit of water out. The capillary pressure goes to infinity at the connate water saturation. This is an indication that for the Agbada reservoir sandstone, with oil/water system, the initial water saturation will decrease with capillary pressure when the reservoir is initially at capillary/gravity equilibrium. Therefore, the cumulative oil production will increase with the decrease in initial water saturation. This means that oil recovery rate in the reservoir will increase with decrease in water saturation. Increase in capillary pressure decreases the formation water saturation thereby increasing the resistivity values for the Formation. This means that with burial, compaction and therefore induration, much of the water is squeezed out of the sediment thereby making the Agbada Formation more resistive to electrical current that would be flowing through it. With values of bulk volume of water being constant or nearly constant for core plugs, it is said to be at irreducible water saturation, inplying that the reservoir in this state can produce water free hydrocarbon as a very good hydrocarbon reservoir.

Porosity of a rock is the measure of its ability to hold a fluid. Permeability on the other hand is a measure of the ease of flow of fluid through a porous solid. However, results have shown that an increase in capillary pressure impact negatively on the samples as both values are decreased which will bring about an increase in cementation and compaction.

REFERENCES

Avbovbo, A. A. (1978) Tertiary lithostratigraphy of the Niger Delta. *American Association of Petroleum Geologists Bulletin*, **62**: 295-300.

Avuru, A., Adeleke, V. and Gbadamosi, T. (2011) Unraveling the structural complexity of the marginal field-The Asuokpu/Umutu study. *Nigeria Association of Petroleum Explorationist*, **23**: 1-4

Charles, L. Vavra., John G. Kaldi and Robert M. Sneider. (1992) Geological application of Capillary Presure. *American Association of Petroleum Geologists Bulletin*, **76**(6): 840-850.

Chukwu, G.A. (2007) The Niger Delta Complex Basin: stratigraphy, structure and hydrocarbon potential. *Journal of Petroleum Geology,* **14**(1): 211-220.

Colin, McPhee and Izaskun Zubizarreta. (2015) Core analysis: in Development in Petroleum Science. Abstract. Retrieved 17 November, 2019 from https//www.sciencedirect.com

Davis, D. K. and Ethridge, F. G. (1975) Sandstone Compaction and Depositional Environment. *American Association of Petroleum Geologists Bulletin*, **59**:239-264.

Dimri, V. P. and Nimisha Vedanti. (2012) Fractal models in Exploration Geophysics. Handbook of Geophysical Exploration: Seismic Exploration. Retrieved 10 march, 2020 from https//www.sciencedirect.com.

Doust, H. and Omatsola, E. (1990) Niger Delta. In J. D. Edwards and Santogrossi P. A. *American Association Of Petroleum Geologist Memoir* 48 Eds., Divergent/passive margin Basin, Pp. 239-248.

Endres, A. L. and Redman, J. D. (1996) Modeling the electrical properties of porous rocks and soil containing immiscible contaminants. *Journal of Environmental and Engineering Geophysics,* **10**: 105-112.

Evamy, B. D., Harembour, J., Kamerling, P., Knaap, W. A., Molloy, F. A. and Rowlands, P. H. (1978) Hadrocarbon habitat of Tertiary Niger Delta. *American Association Of Petroleum Geologist Bulletin*, **62**: 1-39.

Fanchi, R. John. (2002) Measures of rock-fluid interaction: in shared earth modeling. Retrieved 17 November, 2019 from https//www.sciencedirect.com.

Fanchi, R. John. (2018) Rock-fluid interaction: in principles of Applied Reservoir Simulation. Fourth Edition. Retrieved 17 November, 2019 from https//www.sciencedirect.com.

Fen, S. and Sen, P.N. (1985) Geometrical modeling of conductive and dielectric properties of partially saturated rocks. *Journal of applied physics,* **58**: 3236-3243.

Hosper, J. (1971) The geology of the Niger Delta area, in the Geology of the East Atlantic Continental margin, Great Britain, Institute of Geological Science, Report, **70**(16): 121-141.

Lake, L. W. (1989) Enhanced Oil Recovery, Prentice-Hill, Englewood Cliffs NJ, USA.

Mahmud Noorfadreena and Liu Xianhua. (2017) Optimazing well structure and Trajectories for maximizing oil recovery. Proceedings of the International Confernce on Integrated Petroleum Engineering and Geosciences. Pp. 789-793. OI:10.1007/978-981-10-3650-7_67.

Masalmeh, S. K., Jing, X. D., Van Vart, W., Van Der Weerd, W., Christiansen, S. and Van Dorp, H. (2003).“Impact of SCAL on Carbonate reservoir: how capillary forces can affect field performance predictions”, in proceedings of the International Symposium of the society of Core Analysis (SCA ’03), SCA 2003-36, Pau, France.

Merki, J. P. (1972) Stuctural geology of the Cenozoic Niger Delta, in African geology. Ibadan Nigeria: Ibadan University Press. Pp. 635-646.

Milad, Arabloo., Mohammadhossein Heidara Sureshjani and Shahab Gerami. (2014) A new approach for

Scientia Africana, Vol. 19 (No. 2), August, 2020. Pp 15-28
© Faculty of Science, University of Port Harcourt, Printed in Nigeria *ISSN 1118 – 1931*

analysis of production data from constant production rate wells in gas condensate. *Journal of Natural Gas Science and Technology*. Pp. 17-25.

Ndip, E. A., Agyinyi, C. M., Ntom, M. E. and Oladunjoye, M. A. (2018) Seismic Stratigraphy and Petrophysical Characteristics of Reservoirs of the Agbada Formation in the Vicinity of "Well M", offshore Eastern Niger Delta Basin, Nigeria. *Journal of Geology and Geophysics*, **7**(2): 1-9.

Nwachukwu, J. I. and Chukwurah, P. I. (1986) Organic matters of Agbada Formation, Niger Delta, Nigeria. *American Association of Petroleum Geologist Bulletin,* **70**: 48-55.

Oladotun, A. O., Olugbenga, A. E., Chukwudike, G. O. and Olatunji, A. (2016) Modeling hydrocarbon generation potentials of Eocene source rocks in the Agbada Formation, Northern Delta Depobelt, Niger Delta Basin, Nigeria. *Journal of Petroleum Exploration Production Technology*, 379-388.

Robert, B. Szerbia., George, A. MeMechean., Craig Foster and Stephen, H. Snelgrove. (2006) Electrical and Petrophysical modeling of Ferron sandstone data. *Journal of Geophysics*, **71**(5): 197-210.

Stacher, P. (1995) Present understanding of the Niger Delta hydrocarbon habit, in Oti, M. N. and Portma, G. eds., Geology of Deltas, A.A. Balkema, Rotherdam, Pp. 257-267.

Schlumberger. (1972) Log interpretation manual/principles. Vol. 1: Houston, Schlumberger well services Inc.

Ugbena, K. G., Nwankwo, C. N. and Omali, A. O. (2019) Investigating Electrical Response to Water Saturation of Agbada Sandstone in an X-field Niger Delta, Nigeria. *Geoscience Engineering* Volume LXV, **3**: 26-34. ISSN 1802-5420. DOI 10.35180/gse-2019-0015.

Weber, K. J. and Daukoru, E. (1975) Petroleum geology of the Niger Delta. 9th World Petroleum Congress Proceeding, **2**: 209-221.

Xiao, H. and Suppe, J. (1992). Origin of rollovers. *American Association Of Petroleum Geologist Bulletin,* **76**: 509-629.